TISSUE ENGINEERING: Part A
Volume 26, Numbers 7 and 8, 2020

DOI: 10.1089/ten.tea.2019.0202

termis
Tissue Engineering
& Regenerative Medicine
International Society

***ORIGINAL ARTICLE***

# Wnt-Notch Signaling Interactions During Neural and Astroglial Patterning of Human Stem Cells

Julie Bejoy, MS,* Brent Bijonowski, MS, Mark Marzano, MS, Richard Jeske, BS, Teng Ma, PhD,‡ and Yan Li, PhD



The human brain formation involves complicated processing, which is regulated by a gene regulatory network influenced by different signaling pathways. The cross-regulatory interactions between elements of different pathways affect the process of cell fate assignment during neural and astroglial tissue patterning. In this study, the interactions between Wnt and Notch pathways, the two major pathways that influence neural and astroglial differentiation of human induced pluripotent stem cells (hiPSCs) individually, were investigated. In particular, the synergistic effects of Wnt-Notch pathway on the neural patterning processes along the anterior–posterior or dorsal–ventral axis of hiPSC-derived cortical spheroids were explored. The human cortical spheroids derived from hiPSCs were treated with Wnt activator CHIR99021 (CHIR), Wnt inhibitor IWP4, and Notch inhibitor (*N*-[*N*-(3,5-difluorophenacetyl)-l-alanyl]-*S*-phenylglycine *t*-butyl ester [DAPT]) individually, or in combinations (CHIR + DAPT, IWP4 + DAPT). The results suggest that CHIR + DAPT can promote Notch signaling, similar or higher than CHIR alone, whereas IWP4 + DAPT reduces Notch activity compared to IWP4 alone. Also, CHIR + DAPT promoted hindbrain marker HOXB4 expression more consistently than CHIR alone, while IWP4 + DAPT promoted Olig2 expression, indicating the synergistic effects distinctly different from that of the individual small molecule. In addition, IWP4 simultaneously promoted dorsal and ventral identity. The patterned neural spheroids can be switched for astroglial differentiation using bone morphogenetic protein 4. This study should advance the derivations of neurons, astroglial cells, and brain region-specific organoids from hiPSCs for disease modeling, drug screening, as well as for hiPSC-based therapies.

**Keywords:** pluripotent stem cells, neural patterning, spheroids, Wnt, Notch, astroglial

### Impact Statement

Wnt signaling plays a central role in neural patterning of human pluripotent stem cells. It can interact with Notch signaling in defining dorsal–ventral and rostral–caudal (or anterior–posterior) axis of brain organoids. This study investigates novel Wnt and Notch interactions (i.e., Wntch) in neural patterning of dorsal forebrain spheroids or organoids derived from human induced pluripotent stem cells. The synergistic effects of Wnt activator or inhibitor with Notch inhibitor were observed. This study should advance the derivations of neurons, astroglial cells, and brain region-specific organoids from human stem cells for disease modeling and drug screening, as well as for stem cell-based therapies. The results can be used to establish better *in vitro* culture methods for efficiently mimicking *in vivo* structure of central nervous system.

### Introduction

The development of a multicellular organ (such as the brain) from stem cells involves complicated processing.[1,2] Proliferating stem cells undergo the fate decision process before developing into tissues or organs. This process is controlled and regulated by a signaling pathway network (called gene regulatory network).[3] The network comprises pathways created by the intrinsic and extrinsic factors of the cells, which form the signal transduction to control stem cell fate. There are various signal pathways that have been discovered and studied for tissue development and patterning, including Wnt signaling,[4] Notch, and receptor tyrosine kinase.[5–7] It has been suggested that

Department of Chemical and Biomedical Engineering, FAMU-FSU College of Engineering, Florida State University, Tallahassee, Florida.
*Current affiliation: College of Medicine, Vanderbilt University, Nashville, Tennessee.
‡The author passed away unexpectedly on May 18, 2019, due to heart attack.

cross-regulatory interactions between elements of the pathways (e.g., Wnt and Notch) affect the process of cell fate assignment.[8,9] Most components of Wnt signaling have multiple interactions with other signaling pathways (e.g., Hippo/YAP and Notch) and, therefore, have been considered the center of the integrated network.[10] For example, Wnt signaling plays an important role in defining dorsal–ventral (D–V) and rostral–caudal (or anterior–posterior [A–P]) axis of brain organoids together with sonic hedgehog pathway.[11]

The implications on neural differentiation processes from Wnt signaling interacting with other signaling pathways remain largely unexplored. However, several studies revealed major cross-interactions between Wnt and Notch signaling and explained this interaction as integrated control elements of the cells.[12–15] For example, Notch signaling promotes Wnt expression in *Drosophila* development.[5,12] After Wnt refines its expression, it promotes the expression of Notch Ligands (Delta), forming a positive feedback loop to maintain Notch signaling and Wnt expression. A similar mechanism exists for early germ layer specification, where Wnt signaling activates the expression of Notch ligands. Wnt-receptor binding triggers the suppression of the antagonistic activity of Notch. It is also suggested that Wnt performs prepatterning and Notch perform, lateral inhibition. Wnt and Notch pathways control neuronal and astroglial differentiation, in which Notch may not be a primary inducer, but a transit amplifier during neural fate induction, producing simultaneous and synergistic effects (''Wntch'' signaling).

Wnt signaling has been studied for its influence on cardiac and neural differentiation of induced pluripotent stem cells (iPSCs).[16–18] The influence of Wnt signaling on the fate decision of stem cells is both concentration and stage dependent.[19] During early-stage ectoderm differentiation from PSCs, inhibition of Wnt signals was found to promote anterior character and enhance neuroectodermal differentiation.[20] During late-stage neural differentiation, Wnt signaling enriches neural progenitor cells (NPCs) with a posterior neural fate expressing the markers for hindbrain and spinal cord.[17] On the other hand, Notch signaling keeps the neural precursors in an undifferentiated state and inhibits neuronal differentiation.[21] Inhibition of Notch signaling using *N*-[*N*-(3,5-difluorophenacetyl)-l-alanyl]-*S*-phenylglycine *t*-butyl ester (DAPT) promotes neurogenesis in hPSC-derived NPCs.[21–23] Notch inhibition was also used in deriving midbrain organoids and dopaminergic neurons.[24] However, despite Wnt and Notch pathways playing a pivotal role in neural differentiation, cross interactions between these two signaling pathways in patterning of human brain organoids remain underexplored.

In this work, functional cross talks between Wnt and Notch signaling as well as their impacts on the neural and astroglial tissue patterning of human induced pluripotent stem cell (hiPSC)-derived cortical spheroids were evaluated. Previous studies reported that the promoting effect of Wnt activation on neurogenesis of human NPCs was based on modulation of Notch target genes.[25,26] These findings prompted us to hypothesize that manipulation of Wnt and Notch signaling may influence the patterning of neural and astroglial tissue along D–V axis and A–P axis of hiPSC-derived neural spheroids. The cross interactions of the Wnt-Notch signaling were examined using Wnt activator CHIR99021 and Wnt inhibitor IWP4.[27] The resulting influence on Notch and its proneurogenic effect was investigated. At the same time, the impact of Notch inhibition using DAPT on the Wnt signaling and the synergistic effects with CHIR99021 or IWP4 on the neural and astroglial tissue patterning were examined. Understanding these underlying mechanisms that regulate neural and astroglial differentiation and patterning from hiPSCs is essential for efficient derivations of neurons, astroglial cells, and brain region-specific organoids from hiPSCs used in disease modeling, drug screening, and hiPSC-based therapies.

## Materials and Methods

### *Undifferentiated hiPSC culture*

Human iPSK3 cells were derived from human foreskin fibroblasts transfected with plasmid DNA encoding reprogramming factors OCT4, NANOG, SOX2, and LIN28 (kindly provided by Dr. Stephen Duncan, Medical College of Wisconsin).[28,29] Human iPSK3 cells were maintained in mTeSR serum-free medium (StemCell Technologies, Inc., Vancouver, Canada) on growth factor reduced Geltrex-coated surface (Life Technologies).[30] The cells were passaged by Accutase every 5–6 days and seeded at $1 \times 10^6$ cells per well of a six-well plate in the presence of 10 μM Y27632 (Sigma) for the first 24 h.[25,30,31]

### *Cortical spheroid formation from hiPSCs*

Human iPSK3 cells were seeded into ultra-low attachment 24-well plates (Corning Incorporated, Corning, NY) at $3 \times 10^5$ cells/well in a differentiation medium composed of Dulbecco's modified Eagle medium/Nutrient Mixture F-12 plus 2% B27 serum-free supplement (Life Technologies). Y27632 (10 μM) was added during the seeding and removed after 24 h. On day 1, the cells formed embryoid bodies and were treated with dual SMAD signaling inhibitors 10 μM SB431542 (Sigma) and 100 nM LDN193189 (Sigma).[32,33] After 8 days, the cells were treated with fibroblast growth factor-2 (10 ng/mL; Life Technologies) and retinoic acid (5 μM; Sigma) until day 16.[34] At day 17, the spheroids were replated to Geltrex-coated tissue culture plates.

### *Wnt activation, inhibition, and Notch inhibition*

During day 16–21, the spheroids were treated with six different conditions: (i) control, no small molecule was used; (ii) CHIR99021 (10 μM; StemCell Technologies, Inc.), which activates Wnt signaling by inhibiting glycogen synthase kinase-3β; (iii) IWP4 (5 μM; Stemgent, Cambridge, MA), which inhibits Wnt signaling through the porcupine, thereby reducing the production of Wnt proteins[35]; (iv) the Notch inhibitor DAPT (10 μM; Sigma). The γ-secretase inhibitor DAPT can inhibit the γ-secretase-dependent S3 cleavage of Notch, which releases the Notch internal cytoplasmic domain NICD[36,37]; (v) CHIR99021 + DAPT; and (vi) IWP4 + DAPT (Supplementary Fig. S1). The six conditions were labeled as follows: Control, CHIR, IWP4, DAPT, C + D, and I + D. After the treatments, the cells were harvested for immunostaining, flow cytometry, Western blot, or RNA isolation.

For astroglial spheroid differentiation, on day 16, the spheroids were treated with four conditions: (i) control, no factor was used; (ii) bone morphogenetic protein (BMP)-4 at 10 ng/mL (R&D Systems); (iii) IWP4; and (iv) DAPT, up to

day 32 to evaluate the effect of BMP-4 on astroglial fate decision. To elucidate the influence of regional identity of neural progenitors on astroglial differentiation, the spheroid cells (day 21) in the above six conditions were switched to BMP-4 treatment up to day 32. The cells were harvested for characterization of astroglial progenitor markers and brain regional identity markers (Supplementary Figs. S1 and S2).

### *Immunocytochemistry*

Briefly, the samples were fixed with 4% paraformaldehyde (PFA) and permeabilized with 0.2–0.5% Triton X-100. The samples were then blocked for 30 min and incubated with various mouse or rabbit primary antibodies (Supplementary Table S1) for 4 h. After washing, the cells were incubated with the corresponding secondary antibody: Alexa Fluor® 488 goat anti-Mouse $IgG_1$, Alexa Fluor 594 goat anti-Rabbit IgG, or 594 donkey anti-goat IgG (Life Technologies) for 1 h. The samples were counterstained with Hoechst 33342 and visualized using a fluorescent microscope (Olympus IX70, Melville, NY) or a confocal microscope (Zeiss LSM 880). The images from five independent fields (800–1000 cells) were analyzed using ImageJ software. The intensity was calculated based on the area of marker of interest normalized to the nuclei, indicating the relative expression among different conditions.[32,38]

### *Flow cytometry*

To quantify the levels of various neural marker expression, the cells were harvested by trypsinization and analyzed by flow cytometry.[39] Briefly, $1 \times 10^6$ cells per sample were fixed with 4% PFA and washed with staining buffer (2% fetal bovine serum in phosphate-buffered saline [PBS]). The cells were permeabilized with 100% cold methanol, blocked, and then incubated with various primary antibodies (Supplementary Table S1) followed by the corresponding secondary antibody Alexa Fluor 488 goat anti-Mouse $IgG_1$ or Alexa Fluor 594 Goat Anti-rabbit or Donkey Anti-Goat IgG. The cells were acquired with BD FACSCanto™ II flow cytometer (Becton Dickinson) and analyzed against isotype controls using FlowJo software.

### *Western blotting*

Cells were pelleted, washed with ice-cold PBS, and lysed in a hypotonic buffer containing 20 mM HEPES (pH 7.4), 10 mM KCl, 2 mM $MgCl_2$, 1 mM ethylenediaminetetraaceticacid, 1 mM ethylene glycol-bis(β-aminoethyl ether)-N,N,N′,N′-tetraacetic acid, and 1% fresh dithiothreitol. The lysate was centrifuged at 800 *g* for 5 min. NP-40 buffer was added to lyse and resuspend the pellet. Protein concentration of the lysed samples was determined by Bradford assay, and 20 μg of each sample was resolved on a 10% running/4% stacking sodium dodecyl sulfate–polyacrylamide gel electrophoresis gel for 20 min at 100 V and then at 200 V until the end. Proteins were then transferred onto nitrocellulose membranes at 100 V for 1 h. Then the blots were blocked with 3% milk Tris-buffered saline-Tween 20 (TBST) solution for 30 min. After blocking, blots were probed with 0.05 μg/mL of Notch-1, Hes-1, Jagged-1, β-catenin, and so on (Supplementary Table S1), or 1:10,000 β-tubulin (endogenous control) antibody in 3% milk/TBST overnight at 4°C. After washing with TBST, each blot was incubated with 1:10,000 anti-rabbit or anti-mouse Li-Cor (Linclon, NE) infrared secondary antibody for one hour. Finally, blots were washed with TBST and imaged on a Li-Cor Odyssey imager. The relative band intensity was quantified using ImageJ. The average values and standard variations from three blots were presented.

### *Reverse transcription–polymerase chain reaction analysis*

Total RNA was isolated from neural cell samples using the RNeasy Mini Kit (Qiagen, Valencia, CA) according to the manufacturer's protocol followed by the treatment of DNA-Free RNA Kit (Zymo, Irvine, CA). Reverse transcription was carried out using 2 μg of total RNA, anchored oligo-dT primers (Operon, Huntsville, AL), and Superscript III (Invitrogen, Carlsbad, CA) (according to the protocol of the manufacturer). Primers specific for target genes (Supplementary Table S2) were designed using the software Oligo Explorer 1.2 (Genelink, Hawthorne, NY). The gene β-actin was used as an endogenous control for normalization of expression levels. Real-time reverse transcription–polymerase chain reaction analysis (RT-PCR) reactions were performed on an ABI7500 instrument (Applied Biosystems, Foster City, CA), using SYBR1 Green PCR Master Mix (Applied Biosystems). The amplification reactions were performed as follows: 2 min at 50°C, 10 min at 95°C, and 40 cycles of 95°C for 15 s and 55°C for 30 s, and 68°C for 30 s. Fold variation in gene expression was quantified by means of the comparative Ct method: $2^{-(\Delta C_{t\ treatment} - \Delta C_{t\ control})}$, which is based on the comparison of expression of the target gene (normalized to the endogenous control β-actin) among different conditions.

### *$Ca^{2+}$ signaling assay*

For calcium signaling, the samples were replated on 1% Geltrex-coated 96-well plate and grown overnight. The growth medium was removed in each well and 100 μL of 1 × Fluo-4 dye (Life Technologies) in assay buffer containing 1 × Hank's balanced salt solution and 20 mM HEPES (with 2.5 mM probenecid) was added into the wells and incubated at 37°C for 30 min. The incubation was switched to room temperature for an additional 30 min. Baseline $Ca^{2+}$ signals ($I_{494}/I_{516}$) were measured for more than 100 s, and then the calcium dye medium was replaced with 100 μL of 10 μM adenosine 5′-diphosphate (ADP; Sigma) solution in assay buffer (without probenecid). $Ca^{2+}$ recordings were read on a fluorescent plate reader (FLX800; Bioinstrument, Inc., Winooski, VT) using instrument settings appropriate for excitation at 494 nm and emission at 516 nm.

### *Statistical analysis*

The representative experiments were presented and the results were expressed as (mean ± standard deviation). To assess the statistical significance, one-way analysis of variance followed by Fisher's Least Significance Difference *post hoc* tests were performed. A $p$-value $<0.05$ was considered statistically significant.

## Results

### *Effects of Wnt and Notch modulators on Wnt-Notch signaling*

Effects of Wnt and Notch modulators on the expression of β-catenin (a critical protein in canonical Wnt signaling) and

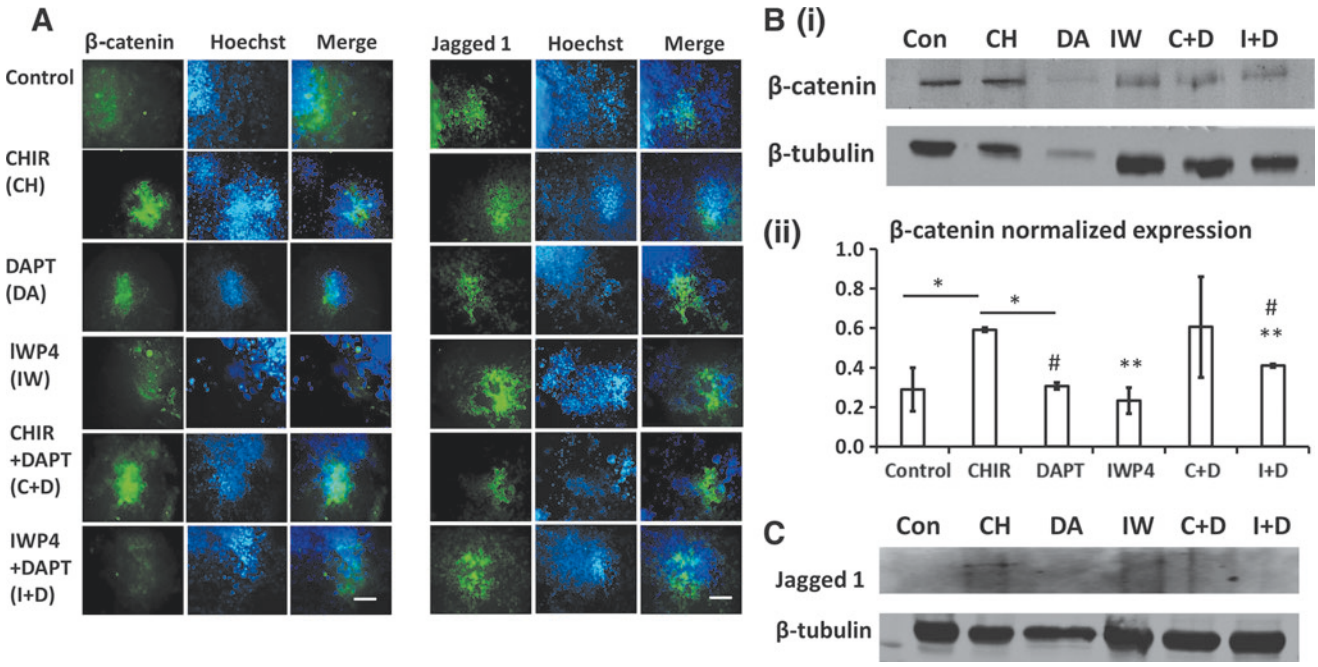


**FIG. 1.** Effects of Wnt and Notch modulators on the expression of β-catenin and Notch ligand Jagged 1 (Wnt-Notch interactions). The neural spheroids were treated with different Wnt and Notch modulators on day 16 and were analyzed for expression of β-catenin and Jagged 1. **(A)** Fluorescent images of β-catenin and Jagged 1. Scale bar: 100 μm. **(B) (i)** Representative Western blots of β-catenin; **(ii)** β-catenin Western blot quantification (normalized expression) using averages from different experimental repeats ($n = 3$). **(C)** Western blots of Jagged 1 expression. *, **, and # indicate $p < 0.05$. Color images are available online.



Notch ligand Jagged 1 (Wnt-Notch interactions) were first evaluated (Fig. 1). The immunocytochemical analysis showed that the expression of β-catenin for the DAPT and IWP4 conditions was reduced compared to the CHIR condition, but was similar to the control condition (Fig. 1A). The CHIR treatment increased the expression of β-catenin compared to the control. Quantification using Western blotting also showed the increased β-catenin expression for the CHIR condition, indicating the activated canonical Wnt signaling. The β-catenin expression in the other four conditions (DAPT, IWP4, C + D, and I + D) was not significantly different from the control condition (Fig. 1B[i], [ii]). The I + D condition had higher β-catenin expression than IWP4 alone or DAPT alone. The impact of Wnt and Notch modulators on the expression of Jagged 1 was also examined using Western blotting. CHIR treatment increased the expression of Jagged 1 compared to the control, whereas all other modulators did not show a significant effect on Jagged 1 (Fig. 1C and Supplementary Fig. S3).

The expression of Notch-1 was evaluated by immunostaining, RT-PCR, and Western blotting (Fig. 2). From RT-PCR analysis, C + D had higher Notch-1 expression than CHIR alone or DAPT alone (Fig. 2B). I + D had lower Notch-1 expression than IWP4 alone, which had the highest Notch-1 expression. From Western blotting analysis, a similar trend for Notch-1 protein was observed (Fig. 2C). C + D had higher Notch-1 expression than CHIR alone, and I + D had lower Notch-1 expression than IWP4 alone. The Notch downstream target protein Hes1 was also evaluated (Fig. 2C). CHIR treatment increased the Hes1 expression compared to the control, indicating high Notch activity. The IWP4 and C + D conditions had high Hes1 expression, consistent with Notch-1. These results suggest that the C + D can induce Notch signaling, similar or higher than CHIR alone, and the I + D reduces Notch activity compared to IWP4 alone, indicating synergistic effects of Wnt signaling and Notch signaling.

The response of YAP localization to Wnt and Notch modulators was qualitatively evaluated (Fig. 2A). Nuclear localization of YAP was observed for the CHIR condition, while more cytoplasmic YAP localization was found for IWP4 treatment. C + D group showed more cytoplasmic YAP than the CHIR group, with I + D group also showing the intermediate level of cytoplasmic YAP. As Hippo/YAP signaling also interacts with Notch signaling (i.e., YAP regulates epidermal stem cell differentiation through Notch inhibition),[40] the three-way interactions of Wnt-Notch-YAP is not surprising.

### *Effects of Wnt and Notch modulators on neural patterning of hiPSCs*

It was hypothesized that Wnt and Notch signaling pathways affect A–P identity (ranging from the telencephalon to the spinal cord) and D–V identify of neural patterning from hiPSCs. Therefore, the analysis of different brain regional markers was performed. Markers correlating with the A–P axis were evaluated, including FOXG1 (A), TBR1 (A), OTX2 (P), and HOXB4 (P) proteins (Fig. 3).[41] The D–V identity was indicated by TBR1 (D), Nkx2.1 (V), and PROX1 (V). On day 25, cells expressing deep-layer VI cortical marker TBR1 were observed. $TBR1^+$ cells were

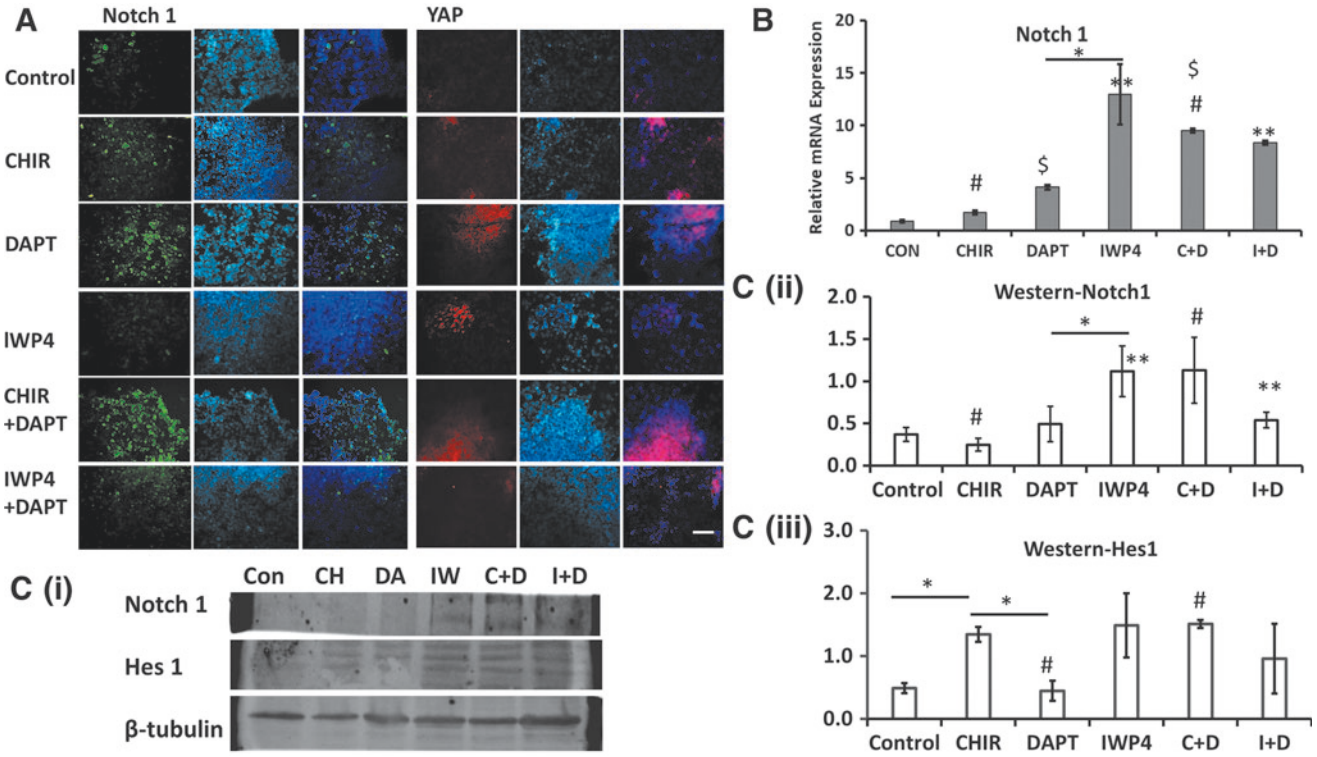


**FIG. 2.** Effects of Wnt and Notch modulators on the expression of Notch receptor Notch-1 and YAP localization (Notch-YAP interactions). The neural spheroids treated with different Wnt and Notch modulators were analyzed for Notch-1 expression and YAP localization. **(A)** Fluorescent images of Notch-1 and YAP. Scale bar: 100 μm. **(B)** RT-PCR analysis of Notch-1 mRNA expression ($n = 3$). **(C) (i)** Western blots of the Notch-1 transmembrane segment and Notch-targeted Hes 1 expression. Western blot quantification (normalized expression) for **(ii)** Notch-1 and **(iii)** Hes 1 proteins ($n = 3$). *, **. #, and $ indicate $p < 0.05$. RT-PCR, reverse transcription–polymerase chain reaction analysis. Color images are available online.

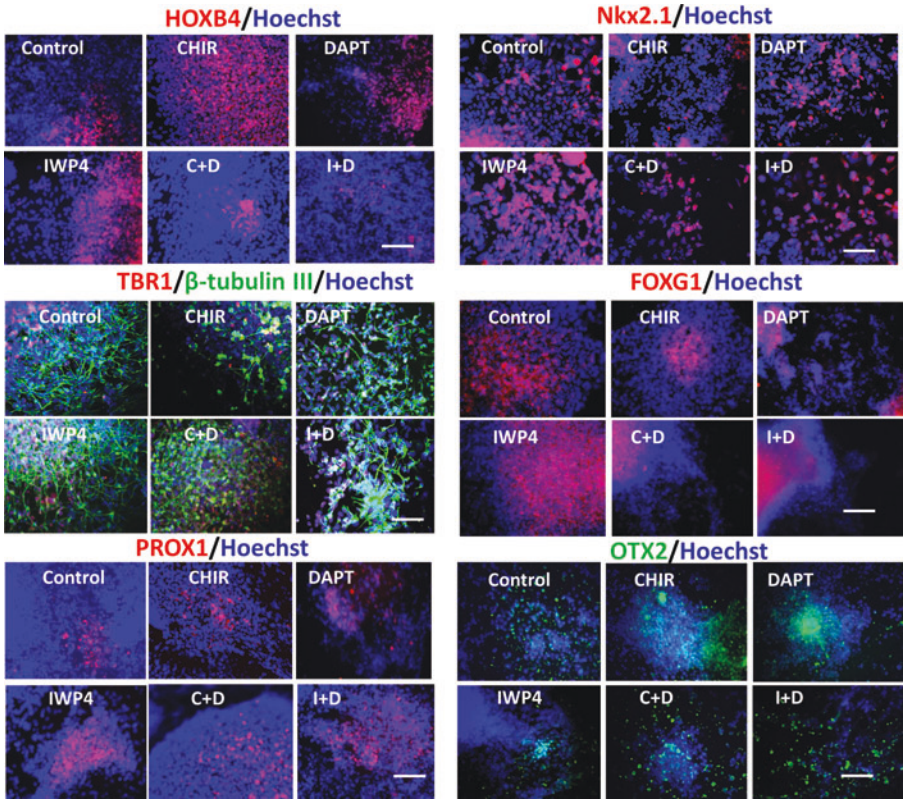


**FIG. 3.** Impacts of Wnt and Notch modulation on neural tissue patterning of hiPSCs. The neural spheroids treated with Wnt and Notch modulators on day 16 were analyzed for different brain regional markers. Fluorescent images of different markers (at day 20): dorsal forebrain-FOXG1; dorsal cortical layer IV-TBR1; hippocampal marker-PROX1; ventral marker-Nkx2.1; midbrain/hindbrain marker-OTX2, hindbrain marker-HOXB4. Scale bar: 100 μm. The six conditions were labeled as follows: Control, CHIR (C), IWP4 (I), DAPT (D), C + D, and I + D. hiPSC, human induced pluripotent stem cell; DAPT, *N*-[*N*-(3,5-difluorophenacetyl)-l-alanyl]-*S*-phenylglycine *t*-butyl ester. Color images are available online.

increased by IWP4 treatment compared to the control (Fig. 3). The expression of ventral forebrain marker Nkx2.1 was also increased using IWP4.

Quantification of HOXB4, TBR1, and Nkx2.1 was performed using flow cytometry (Fig. 4A). For HOXB4, C + D (66.6 ± 8.3%) and CHIR (65.9 ± 7.6%) conditions had the highest expression, while all other conditions were comparable to the control. C + D had higher expression than DAPT alone, while I + D showed lower expression than DAPT alone. For TBR1, IWP4 (70.9 ± 2.9%) and DAPT (65.2 ± 7.1%) conditions had the highest expression. C + D had lower expression than DAPT alone or CHIR alone, while I + D had lower TBR1 expression than DAPT alone or IWP4 alone. The control condition had the lowest expression (35.0 ± 8.8%). For Nkx2.1, the highest expression was observed for IWP4 (53.5 ± 7.0%), C + D (55.6 ± 8.7%), and CHIR (52.4 ± 2.2%) conditions. In addition, C + D had higher expression than DAPT alone. The representative flow cytometry histograms are shown in Figure 4B.

Flow cytometry was also performed for FOXG1 (A), the forebrain marker, and Olig2 (P, V), the hindbrain marker expressed in motor neuron progenitors, cerebellar progenitors, and spinal oligodendrocyte progenitors (Fig. 5A).[42] CHIR reduced the level of FOXG1, whereas IWP4 treatment upregulated FOXG1. For Olig2, CHIR had the highest expression (22.3%), while the other conditions had low expression (10.9–21.9%). Since the promoting effects of IWP4 on forebrain markers (A, D) were definitive, but the effects of CHIR on hindbrain markers were inconsistent, another midbrain/hindbrain marker OTX2 was included. Western blotting was performed for OTX2 and Olig2, as well as HOXB4 and TBR1 (Fig. 5B). For HOXB4, CHIR and IWP4 had the highest expression. C + D reduced the expression compared to CHIR, and I + D reduced the expression compared to IWP4 alone. For OTX2, CHIR condition had the highest expression. C + D group had lower expression than CHIR, and the I + D group had lower expression than IWP4 alone. For Olig2, the highest expression was observed for I + D condition. The trend of TBR1 expression using Western blotting was consistent with flow cytometry results.

RT-PCR analysis was performed for mRNA expression of HOXB4, TBR1, Nkx2.1, and Olig2, as well as hindbrain cerebellar genes NEPH3 and MATH1 (Fig. 6). For HOXB4, the highest expression was observed for IWP4 condition (2.64 ± 0.04), followed by C + D (2.18 ± 0.01) and I + D (1.95 ± 0.35) conditions. The expression for C + D condition was higher than CHIR alone or DAPT alone. For TBR1, the highest expression was also observed for IWP4 condition (16.89 ± 1.68), followed by C + D (14.28 ± 1.07) and I + D (6.89 ± 0.52) conditions. The expression for C + D condition was again higher than CHIR alone or DAPT alone. Similarly, for Nkx2.1, the highest expression was observed for IWP4 condition (14.95 ± 0.36), followed by C + D (9.23 ± 0.54) and I + D (9.48 ± 0.36). However, for Olig2, the highest expression was observed for I + D (7.68 ± 0.16) condition, followed by DAPT (3.61 ± 0.17) and IWP4 (3.53 ± 0.62) conditions. The expression for C + D condition was higher than CHIR alone. For hindbrain cerebellar genes NEPH3 and MATH1, the highest expression was observed for IWP4 condition. The inclusion of DAPT with IWP4 reduced the expression significantly.

PAX6 is expressed dorsally in the forebrain. I + D reduced the expression of PAX6 compared to IWP4 alone, suggesting the reduction of anterior dorsal phenotype (Supplementary Fig. S4). The basic helix-loop-helix transcription factor PTF1a is expressed by ventricular zone of the cortical plate. PTF1a$^+$ progenitors have been reported to generate GABAergic neurons of cerebellar cortex (Purkinje cells and interneurons).[43] The highest PTF1a expression was observed for the C + D condition (33.4%), while other conditions had low expression (1.4–20.8%), probably due to the early developmental stage (Supplementary Fig. S4). The general neural markers Nestin and β-tubulin III were also evaluated (Supplementary Fig. S5). C + D (42.1%) and CHIR (39.6%) conditions had the highest Nestin expression, while the other conditions had 20.7–37.0% of Nestin$^+$ cells. The β-tubulin III$^+$ cells were the most for CHIR (87.5%) and I + D (89.8%) conditions, while the other conditions had 52.1–56.9%.

Taken together, these data indicate the synergistic effects of C + D and I + D on A–P and D–V axis patterning of hiPSCs compared to CHIR, IWP4, or DAPT alone. IWP4 alone promoted forebrain marker expression (dorsal and ventral) and HOXB4 gene expression. CHIR alone did not consistently promote hindbrain marker HOXB4 expression, but it reduced FOXG1 expression. C + D promoted hindbrain marker HOXB4 expression, while I + D promoted Olig2 expression.

### *Effects of Wnt and Notch modulators on astroglial patterning of hiPSCs*

Neurons and astrocytes originate from the same neuroepithelial cells in vertebrates where astrogliogenesis follows neurogenesis. The gliogenic switch can be obtained using Notch activating molecules and cytokines such as BMP4.[1,44] Our hypothesis is that hiPSC-derived neural spheroids that undergo tissue patterning using Wnt-Notch modulators should switch to the fate of astroglial cells with the corresponding brain regional identity under BMP4 treatment. In this study, the effects of BMP4 on GFAP and S100β expression (co-localized with TBR1 and HOXB4) were observed (Supplementary Figs. S6 and S7). Then, the cells of the six conditions were changed to BMP4 treatment after day 20 and the day 32 cells were analyzed for markers of developing astrocytes, including GFAP, Aldolase C, S100β, and vimentin (Fig. 7). The quantification of Western blot showed that for GFAP, the highest expression was observed for the CHIR group. All other groups had lower expression than the control condition (BMP4 only). The expression in the C + D group was lower than the CHIR condition, and the I + D group had lower expression than the IWP4 group. For S100β, the DAPT, C + D, and I + D groups had lower expression than the control condition, while the CHIR and IWP4 groups had similar expression. For vimentin, the IWP4 condition had lower expression than the control, while all other conditions were similar to the control. For Aldolase C, all the groups had comparable expression to the control. C + D and DAPT groups had lower expression than CHIR alone. The flow cytometry results of GFAP confirmed the presence of astrocytes (Supplementary Fig. S8). The co-localization of FOXG1/GFAP, HOXB4/GFAP, and Nkx2.1/GFAP indicates that astroglial cells generated in each

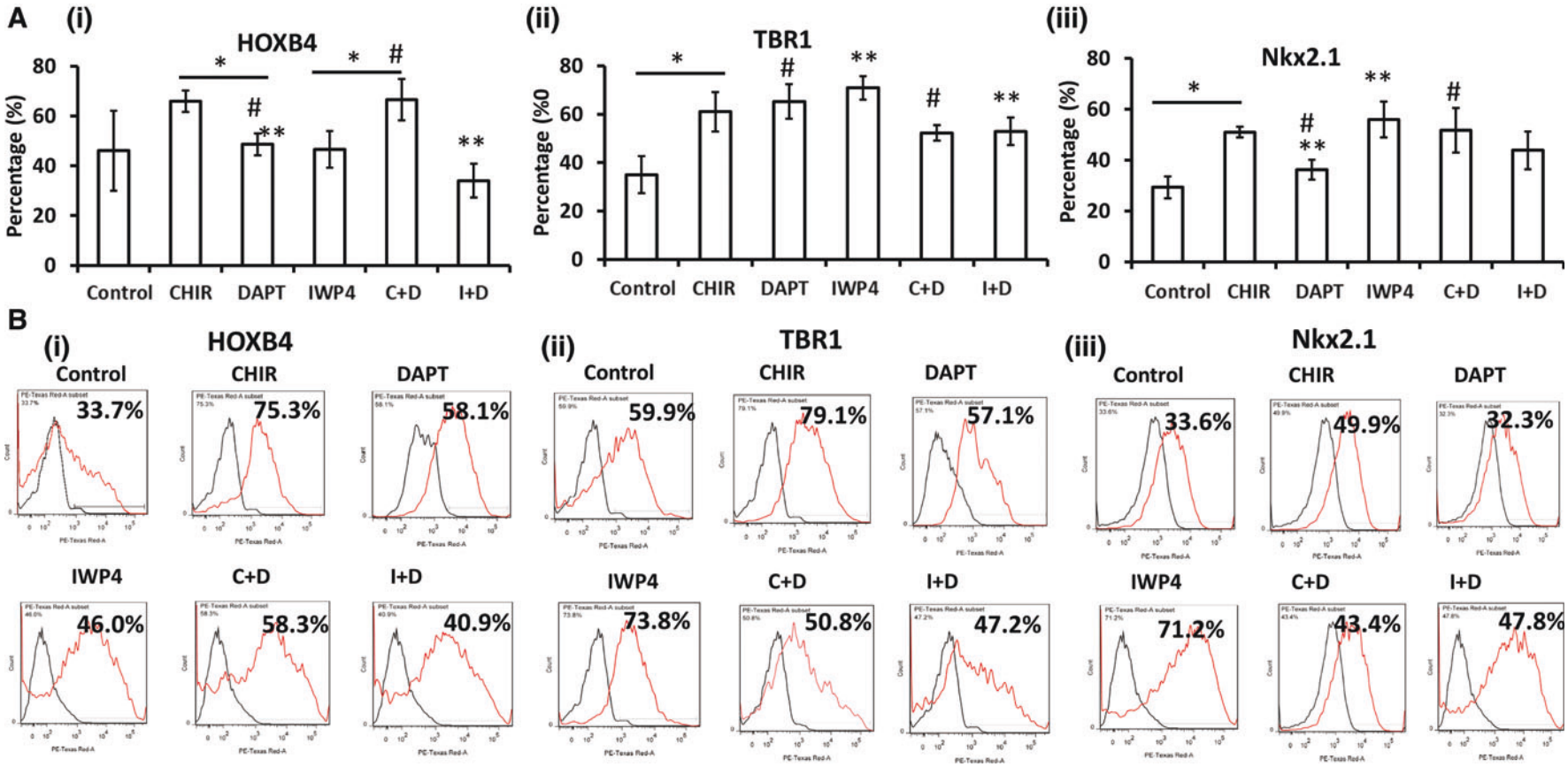


**FIG. 4.** Quantification of brain regional marker expression of neural spheroids derived from hiPSCs. The neural spheroids treated with Wnt and Notch modulators on day 16 were analyzed using flow cytometry (at day 21). **(A)** Flow cytometry analysis of dorsal forebrain marker TBR1, ventral marker Nkx2.1, and hindbrain marker HOXB4 ($n=3$). **(B)** Representative flow cytometry plots of TBR1, HOXB4, and Nkx2.1. (i) HOXB4; (ii) TBR1; (iii) Nkx2.1. *Black line*: negative control; *Red line*: marker of interest. *, **, and # indicate $p<0.05$. Color images are available online.

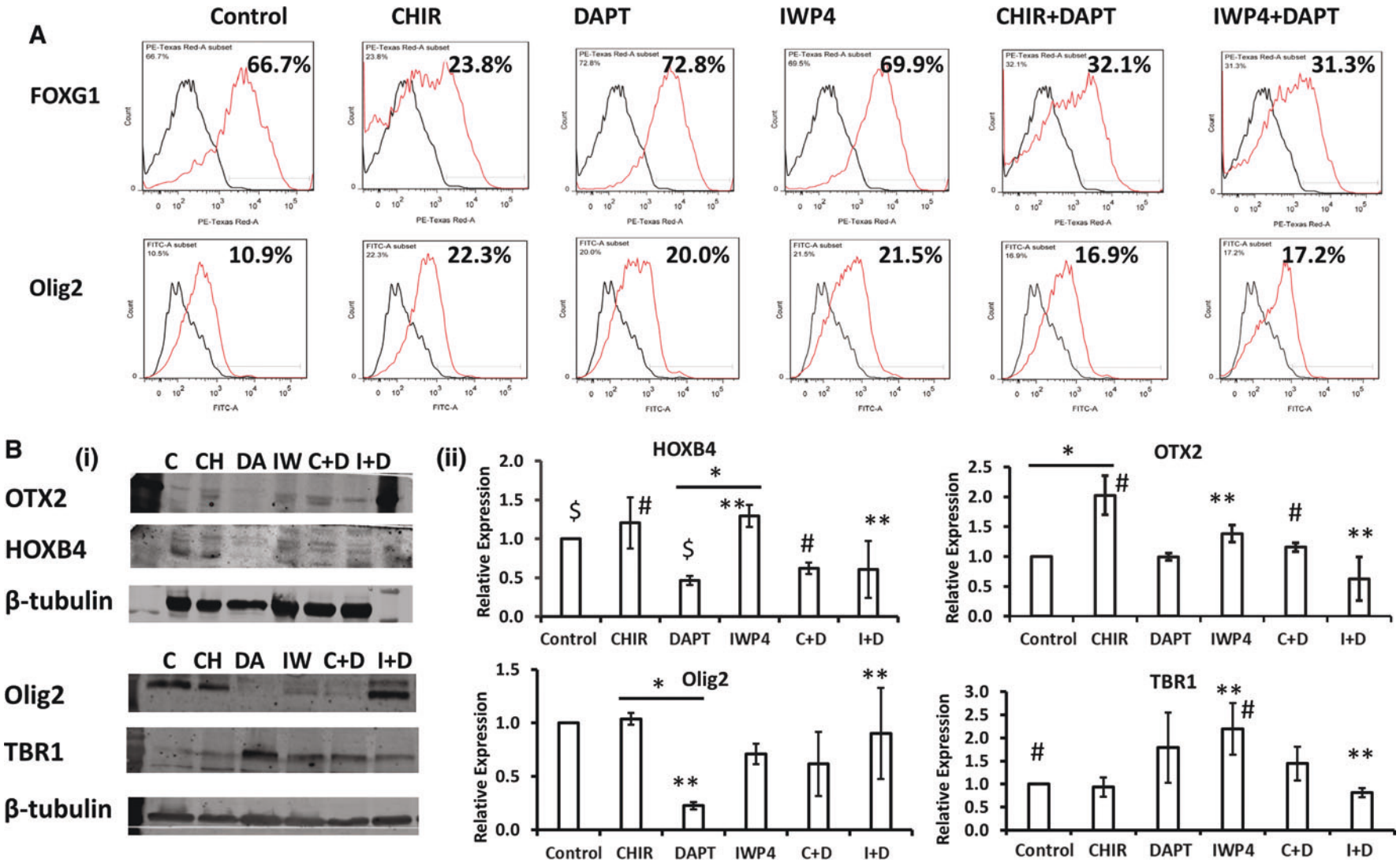


**FIG. 5.** Additional brain regional marker expression of neural spheroids derived from hiPSCs. **(A)** Flow cytometry plots of FOXG1 and additional hindbrain/midbrain marker (Olig2) on day 21. *Black line*: negative control; *Red line*: marker of interest. **(B) (i)** Western blots of the brain regional markers HOXB4, OTX2 (hindbrain/midbrain), Olig2, and TBR1; **(ii)** Quantification (normalized expression) of Western blot band density ($n = 3$). The six conditions were labeled as follows: Control, CHIR (C), IWP4 (I), DAPT (D), C + D, and I + D. *, **, #, and $ indicate $p < 0.05$. Color images are available online.

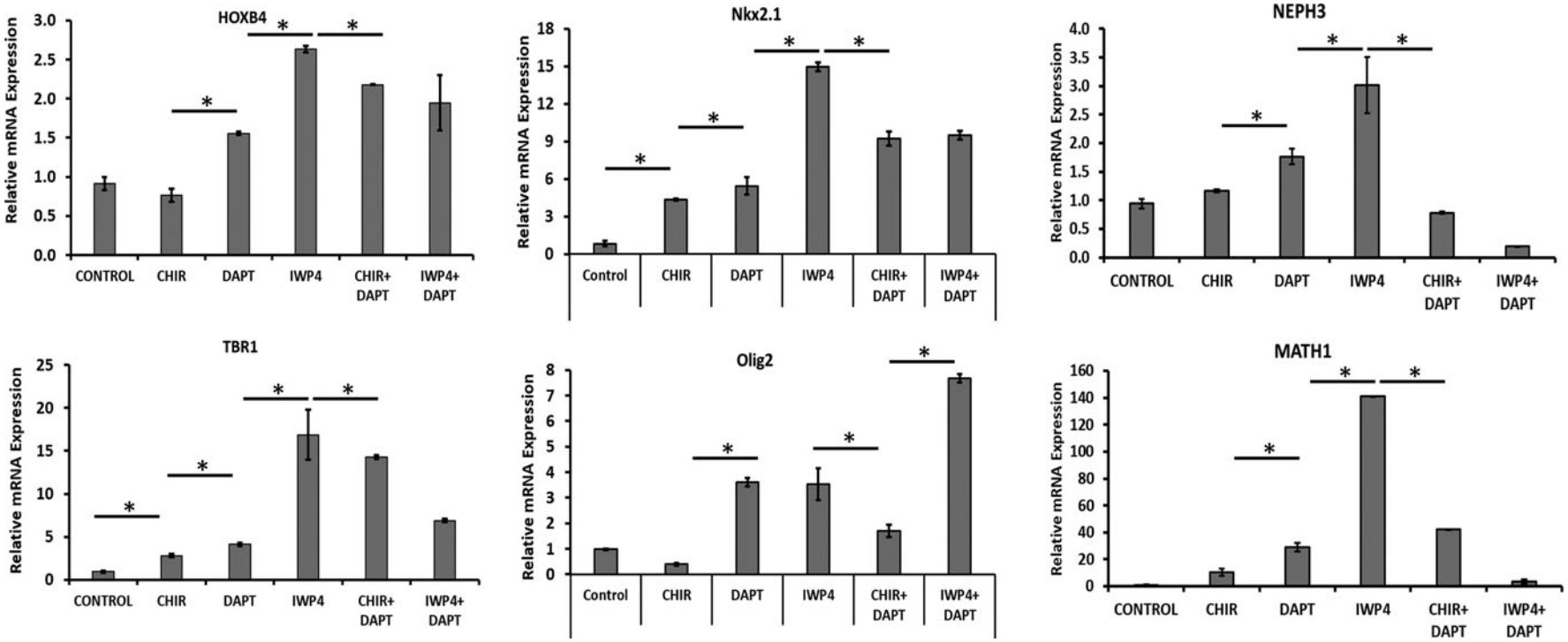


**FIG. 6.** Quantification of brain regional marker mRNA expression using RT-PCR analysis. The neural spheroids treated with Wnt and Notch modulators on day 16 were analyzed using RT-PCR (at day 21). RT-PCR analysis of hindbrain genes (HOXB4 and Olig2), forebrain gene (dorsal-TBR1 and ventral-Nkx2.1), and cerebellar genes (MATH1 and NEPH3) ($n = 3$). The six conditions were labeled as follows: Control, CHIR (C), IWP4 (I), DAPT (D), C + D, and I + D. *$p < 0.05$.

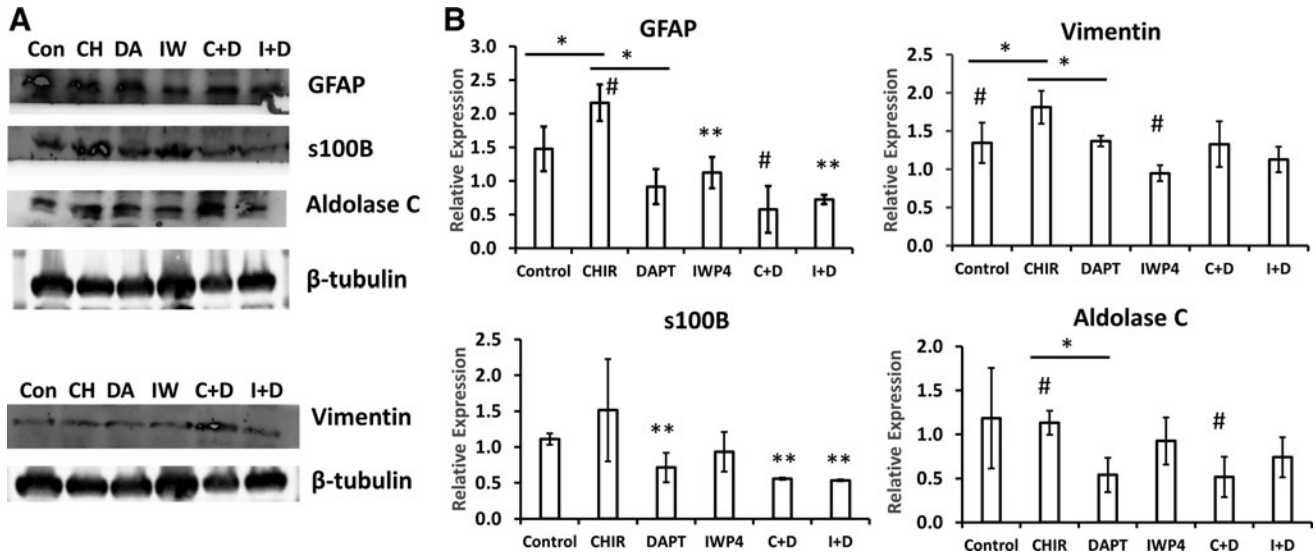


**FIG. 7.** Impacts of Wnt and Notch modulation on astroglial tissue patterning of cortical spheroids when treated with BMP4. **(A)** Western blots of the astrocyte markers GFAP, S100B, V/vimentin, and Aldolase C; **(B)** Quantification (normalized expression) of Western blot band density ($n=3$). The six conditions were labeled as follows: Control, CHIR (C), IWP4 (I), DAPT **(D)**, C + D, and I + D. *, **, and # indicate $p<0.05$. BMP, bone morphogenetic protein.

condition retained the brain regional identity (Supplementary Fig. S9). Our data also suggest that the cultures contained developing astrocytes at different stages of maturity (e.g., Aldolase C is a more mature marker).

Astrocytes express a large collection of metabotropic receptors linked to $Ca^{2+}$ signaling. The activation of these receptors releases $Ca^{2+}$ from intracellular stores. The $Ca^{2+}$ changes in the derived astrocytes were determined using the $Ca^{2+}$ indicator Fluo-4. The baseline calcium transients were measured followed with ADP (100 μM) stimulation. The $Ca^{2+}$ transient images were observed for different groups (Supplementary Fig. S10A). A brief application (400 s) of ADP triggered $Ca^{2+}$ transients in astrocytes with a rapid increase in intracellular $Ca^{2+}$ levels (Supplementary Fig. S10B). Only the I+D group expressed transients lower compared with the control group.

## Discussion

Wnt signaling pathway is one of the major determinants of the brain regional identity of NPCs. D–V patterning of NPCs can be achieved through a coordination of Wnt and sonic hedgehog (Shh) signaling agonists and antagonists.[17,32,45] The cross-regulatory interactions among different pathways, such as Wnt, Hippo/YAP, Notch, and JAK-STAT, affect the process of neurogenesis or gliogenesis from NPCs and accelerate neural differentitaion.[35,46] Wnt signaling was reported to have recurrent interactions with Notch signaling, which is a major pathway to elevate the expression of mature neurons from stem cells.[9,13,15,47] Notch signaling plays a vital role in the neurogenesis of vertebrates and is required for the maintenance of neural stem cells in the embryonic and adult brain.[48–50] Notch was found to regulate the balance between the progenitor pool and neural differentiation, hence preventing premature neurogenesis *in vitro*. The cross-regulatory interactions between Wnt and Notch (i.e., Wntch) can be activating, repressing, or with dynamic Wnt and Notch signaling oscillations,[14] depending on the species and the tissue context. In this study, functional cross-talk between Wnt and Notch signaling on neural and astroglial tissue patterning from hiPSCs was investigated.

Our results demonstrate that the combinational treatments of hiPSC-derived cortical spheroids with Wnt and Notch modulators have synergistic effects compared to the individual factor treatment. Notch inhibition using DAPT did not promote the expression of β-catenin, but the expression was promoted when treated together with CHIR. On the other side, CHIR increased the expression of Notch downstream target Hes1, possibly by upregulating Notch receptor Jagged 1. IWP4 was able to increase Hes1 expression compared to the control by upregulating Notch 1. Even though the DAPT treatment reduced Notch activity, C+D treatment was able to maintain Hes 1 expression, indicating the dominating effect of Wnt activation over the Notch inhibition. However, for I+D treatment, IWP4 was not able to maintain Notch activity in the presence of DAPT, suggesting that Notch inhibition was dominant over Wnt inhibition. These results suggest the possibility of repressing impact of Notch inhibitor DAPT on Wnt inhibition and the positive impact of Wnt activation on Notch signaling.[27]

In our study, combinational treatments of Wnt and Notch modulators affected brain regional identity of iPSC-derived spheroids. Our previous study indicates that Wnt activation with CHIR leads to the higher expression of genes with a hindbrain identity,[25] whereas inhibition of Wnt signaling with IWP4 results in the higher expression of markers with a forebrain phenotype.[51] This study indicates that the addition of DAPT to CHIR or IWP4 influences neural patterning effects of Wnt signaling. Notch inhibition using DAPT reduced the hindbrain $HOXB4^+$ cells compared to the CHIR condition, but the CHIR + DAPT treatment was able to maintain the $HOXB4^+$ cells based on flow cytometry results. For midbrain marker OTX2, CHIR + DAPT treatment reduced the expression compared to CHIR alone. Analysis of

forebrain markers TBR1 and FOXG1 showed that I+D reduced their expression compared to IWP4 alone. I+D also reduced the expression of ventral forebrain marker Nkx 2.1. In addition, I+D treatment was able to increase the gene expression of Olig2 (expressed in motor neuron progenitors, cerebellar progenitors, and spinal oligodendrocyte progenitors), while C+D treatment was not, indicating that Notch inhibition dominates Wnt inhibition. The suggested Notch activation by CHIR reduces the impact of DAPT on brain regional patterning, whereas DAPT reduces the Wnt inhibition effects. Discrepancy in gene and protein expression of Olig2 was observed, possibly due to variability in differentiation, cell-based nature of flow cytometry analysis, and the semiquantitative nature of RT-PCR analysis.

Astrocytes were reported to exist in cerebral organoids and get mature with time (reaching 10–20% in cerebral organoids).[52–54] The major molecules associated with NPC commitment to astroglial cells include Notch molecules, leukemia inhibitory factor, ciliary neurotrophic factor, and BMP4.[1,44] BMPs activate the astrocyte differentiation by suppressing oligodendrocyte differentiation.[55] In the brain, BMPs are secreted from dorsal structures, which then form a gradient, helping to pattern the D—V axis of brain tissue.[56] BMP4 treatment was reported to activate STAT proteins through the serine-threonine kinase FKBP12/rapamycin-associated protein (FRAP). FRAP, in turn, catalyzes phosphorylation of STAT and promotes astrocytic gene expression. Synergic effects of LIF-STAT3 and BMP-Smad signaling promote astrocytic differentiation by activating the GFAP promoter through a STAT3-p300/CBP-Smad1 complex.

In this study, the cortical spheroids were treated with Wnt and Notch signaling modulators and then switched to gliogenesis by BMP4 treatment. Co-existence of neurons and astrocytes was observed in our study. The co-development of neurons, astrocytes, and oligodendrocytes was also reported in a three-dimensional neural spheroid model.[57] Astrocytes have functional diversity in different human brain regions.[58,59] Since the cortical spheroids generated with different Wnt and Notch modulators have different regional identity, our hypothesis is that the astroglial cells produced for each condition modulated by Wnt and Notch signaling should retain the brain regional identity and may possess functional diversity.[60]

Our results indicate that the CHIR group expresses the highest levels of astrocyte markers GFAP and vimentin compared to the other groups, possibly because that CHIR treatment increases Notch activity and Notch ligand expression in the derived cortical spheroids. It was reported that canonical Wnt signaling can transcriptionally activate Notch signaling mediated by CTNNB1.[27] Notch ligand-expressing NPCs can provide feedback signals to the residual Notch-expressing NPCs and activate astrocyte differentiation. The activation of Notch signaling potentiates the differentiation of NPCs into astrocytes, but requires the signals from astrocyte-inducing cytokines for efficient differentiation.[61] So the addition of Notch inhibitor DAPT to CHIR reduced astrocyte marker expression. By contrast, treatment with Wnt inhibitor IWP4 + BMP4 induced the expression of astrocyte markers Aldolase C, S100β, and GFAP, but the expression levels were not up to the level of the BMP4 control group. The addition of DAPT to IWP4 also reduced the astrocyte marker expression. The lowest expression of astrocyte markers was shown in the I+D group, indicating the dominance of DAPT effect over IWP4 effect on astrocyte differentiation.

## Conclusions

In this study, the functional cross-talks between Wnt and Notch signaling during neural and astroglial tissue patterning of hiPSCs were investigated using Wnt and Notch modulators. The results suggest the possibility of repressing effects of Notch inhibitor DAPT on Wnt inhibition and the positive impact of Wnt activation on Notch signaling for brain regional identity of hiPSC-derived cortical spheroids. Taken together, the IWP4 condition is more optimal for enrichment of a balanced population with forebrain or cerebellar fates. The CHIR condition is more optimal for enrichment of population with midbrain or certain hindbrain fate, as well as gliogenesis. This study should advance the derivations of neurons, astroglia, and brain region-specific organoids from human stem cells for disease modeling and drug screening, as well as for stem cell-based therapies.

## Acknowledgments

The authors thank Ms. Ruth Didier of FSU Department of Biomedical Sciences for her help with flow cytometry analysis, Dr. Brian K. Washburn and Kristina Poduch in FSU Department of Biological Sciences for their help with RT-PCR analysis, Dr. Stephen Duncan at Medical College of Wisconsin, and Dr. David Gilbert in FSU Department of Biological Sciences for human iPSK3 cells.

## Disclosure Statement

No competing financial interests exist.

## Funding Information

This work is supported by National Science Foundation Career Award (No. 1652992 to Y.L.).

## Supplementary Material

Supplementary Figure S1
Supplementary Figure S2
Supplementary Figure S3
Supplementary Figure S4
Supplementary Figure S5
Supplementary Figure S6
Supplementary Figure S7
Supplementary Figure S8
Supplementary Figure S9
Supplementary Figure S10
Supplementary Table S1
Supplementary Table S2

## References

1. Tao, Y., and Zhang, S.C. Neural subtype specification from human pluripotent stem cells. Cell Stem Cell **19,** 573, 2016.
2. Suzuki, I.K., and Vanderhaeghen, P. Is this a brain which I see before me? Modeling human neural development with pluripotent stem cells. Development **142,** 3138, 2015.
3. Zhang, X., Peterson, K.A., Liu, X.S., McMahon, A.P., and Ohba, S. Gene regulatory networks mediating canonical

Wnt signal directed control of pluripotency and differentiation in embryo stem cells. Stem Cells **31,** 2667, 2013.
4. MacDonald, B.T., Tamai, K., and He, X. Wnt/beta-catenin signaling: components, mechanisms, and diseases. Dev Cell **17,** 9, 2009.
5. Siebel, C., and Lendahl, U. Notch signaling in development, tissue homeostasis, and disease. Physiol Rev **97,** 1235, 2017.
6. Dontu, G., Jackson, K.W., McNicholas, E., Kawamura, M.J., Abdallah, W.M., and Wicha, M.S. Role of Notch signaling in cell-fate determination of human mammary stem/progenitor cells. Breast Cancer Res **6,** R605, 2004.
7. Lin, F., Shao, Y., Xue, X., et al. Biophysical phenotypes and determinants of anterior vs. posterior primitive streak cells derived from human pluripotent stem cells. Acta Biomater **86,** 125, 2019.
8. Maury, Y., Come, J., Piskorowski, R.A., et al. Combinatorial analysis of developmental cues efficiently converts human pluripotent stem cells into multiple neuronal subtypes. Nat Biotechnol **33,** 89, 2015.
9. Collu, G.M., Hidalgo-Sastre, A., and Brennan, K. Wnt-Notch signalling crosstalk in development and disease. Cell Mol Life Sci **71,** 3553, 2014.
10. Azzolin, L., Panciera, T., Soligo, S., et al. YAP/TAZ incorporation in the beta-catenin destruction complex orchestrates the Wnt response. Cell **158,** 157, 2014.
11. Di Lullo, E., and Kriegstein, A.R. The use of brain organoids to investigate neural development and disease. Nat Rev Neurosci **18,** 573, 2017.
12. Hayward, P., Kalmar, T., and Arias, A.M. Wnt/Notch signalling and information processing during development. Development **135,** 411, 2008.
13. Munoz-Descalzo, S., de Navascues, J., and Arias, A.M. Wnt-Notch signalling: an integrated mechanism regulating transitions between cell states. Bioessays **34,** 110, 2012.
14. Sonnen, K.F., Lauschke, V.M., Uraji, J., et al. Modulation of phase shift between Wnt and Notch signaling oscillations controls mesoderm segmentation. Cell **172,** 1079.e12, 2018.
15. Kessler, M., Hoffmann, K., Brinkmann, V., et al. The Notch and Wnt pathways regulate stemness and differentiation in human fallopian tube organoids. Nat Commun **6,** 8989, 2015.
16. Lian, X., Hsiao, C., Wilson, G., et al. Robust cardiomyocyte differentiation from human pluripotent stem cells via temporal modulation of canonical Wnt signaling. Proc Natl Acad Sci U S A **109,** E1848, 2012.
17. Moya, N., Cutts, J., Gaasterland, T., Willert, K., and Brafman, D.A. Endogenous WNT signaling regulates hPSC-derived neural progenitor cell heterogeneity and specifies their regional identity. Stem Cell Rep **3,** 1015, 2014.
18. Bejoy, J., Wang, Z., Bijonowski, B., et al. Differential effects of heparin and hyaluronic acid on neural patterning of human induced pluripotent stem cells. ACS Biomater Sci Eng **4,** 4354, 2018.
19. Hirsch, C., Campano, L.M., Wohrle, S., and Hecht, A. Canonical Wnt signaling transiently stimulates proliferation and enhances neurogenesis in neonatal neural progenitor cultures. Exp Cell Res **313,** 572, 2007.
20. ten Berge, D., Koole, W., Fuerer, C., Fish, M., Eroglu, E., and Nusse, R. Wnt signaling mediates self-organization and axis formation in embryoid bodies. Cell Stem Cell **3,** 508, 2008.
21. Woo, S.M., Kim, J., Han, H.W., et al. Notch signaling is required for maintaining stem-cell features of neuroprogenitor cells derived from human embryonic stem cells. BMC Neurosci **10,** 97, 2009.
22. Qi, Y., Zhang, X.J., Renier, N., et al. Combined small-molecule inhibition accelerates the derivation of functional cortical neurons from human pluripotent stem cells. Nat Biotechnol **35,** 154, 2017.
23. Borghese, L., Dolezalova, D., Opitz, T., et al. Inhibition of notch signaling in human embryonic stem cell-derived neural stem cells delays G1/S phase transition and accelerates neuronal differentiation in vitro and in vivo. Stem Cells **28,** 955, 2010.
24. Tieng, V., Stoppini, L., Villy, S., Fathi, M., Dubois-Dauphin, M., and Krause, K.H. Engineering of midbrain organoids containing long-lived dopaminergic neurons. Stem Cells Dev **23,** 1535, 2014.
25. Bejoy, J., Song, L., Zhou, Y., and Li, Y. Wnt-Yes associated protein interactions during neural tissue patterning of human induced pluripotent stem cells. Tissue Eng Part A **24,** 546, 2018.
26. Song, L., Yuan, X., Jones, Z., et al. Assembly of human stem cell-derived cortical spheroids and vascular spheroids to model 3-D brain-like tissues. Sci Rep **9,** 5977, 2019.
27. Ma, L., Wang, Y., Hui, Y., et al. WNT/NOTCH pathway is essential for the maintenance and expansion of human MGE progenitors. Stem Cell Rep **12,** 934, 2019.
28. Si-Tayeb, K., Noto, F.K., Sepac, A., et al. Generation of human induced pluripotent stem cells by simple transient transfection of plasmid DNA encoding reprogramming factors. BMC Dev Biol **10,** 81, 2010.
29. Si-Tayeb, K., Noto, F.K., Nagaoka, M., et al. Highly efficient generation of human hepatocyte-like cells from induced pluripotent stem cells. Hepatology **51,** 297, 2010.
30. Yan, Y., Martin, L., Bosco, D., et al. Differential effects of acellular embryonic matrices on pluripotent stem cell expansion and neural differentiation. Biomaterials **73,** 231, 2015.
31. Song, L., Wang, K., Li, Y., and Yang, Y. Nanotopography promoted neuronal differentiation of human induced pluripotent stem cells. Colloids Surf B Biointerfaces **148,** 49, 2016.
32. Yan, Y., Bejoy, J., Xia, J., Guan, J., Zhou, Y., and Li, Y. Neural patterning of human induced pluripotent stem cells in 3-D cultures for studying biomolecule-directed differential cellular responses. Acta Biomater **42,** 114, 2016.
33. Yan, Y., Song, L., Madinya, J., Ma, T., and Li, Y. Derivation of cortical spheroids from human induced pluripotent stem cells in a suspension bioreactor. Tissue Eng Part A **24,** 418, 2018.
34. Nadadhur, A.G., Leferink, P.S., Holmes, D., et al. Patterning factors during neural progenitor induction determine regional identity and differentiation potential in vitro. Stem Cell Res **32,** 25, 2018.
35. Bejoy, J., Song, L., and Li, Y. Wnt-YAP interactions in the neural fate of human pluripotent stem cells and the implications for neural organoid formation. Organogenesis **12,** 1, 2016.
36. Wimmer, R.A., Leopoldi, A., Aichinger, M., et al. Human blood vessel organoids as a model of diabetic vasculopathy. Nature **565,** 505, 2019.
37. Trac, D., Maxwell, J.T., Brown, M.E., Xu, C., and Davis, M.E. Aggregation of child cardiac progenitor cells into spheres activates notch signaling and improves treatment of right ventricular heart failure. Circ Res **124,** 526, 2019.

38. Sart, S., Yan, Y., Li, Y., et al. Crosslinking of extracellular matrix scaffolds derived from pluripotent stem cell aggregates modulates neural differentiation. Acta Biomater **30,** 222, 2016.
39. Sart, S., Ma, T., and Li, Y. Extracellular matrices decellularized from embryonic stem cells maintained their structure and signaling specificity. Tissue Eng Part A **20,** 54, 2014.
40. Totaro, A., Castellan, M., Battilana, G., et al. YAP/TAZ link cell mechanics to Notch signalling to control epidermal stem cell fate. Nat Commun **8,** 15206, 2017.
41. Cederquist, G.Y., Asciolla, J.J., Tchieu, J., et al. Specification of positional identity in forebrain organoids. Nat Biotechnol **37,** 436, 2019.
42. Liu, Y., Jiang, P., and Deng, W. OLIG gene targeting in human pluripotent stem cells for motor neuron and oligodendrocyte differentiation. Nat Protoc **6,** 640, 2011.
43. Muguruma, K., Nishiyama, A., Kawakami, H., Hashimoto, K., and Sasai, Y. Self-organization of polarized cerebellar tissue in 3D culture of human pluripotent stem cells. Cell Rep **10,** 537, 2015.
44. Zhao, J., Davis, M.D., Martens, Y.A., et al. APOE epsilon4/epsilon4 diminishes neurotrophic function of human iPSC-derived astrocytes. Hum Mol Genet **26,** 2690, 2017.
45. Wilson, L., and Maden, M. The mechanisms of dorsoventral patterning in the vertebrate neural tube. Dev Biol **282,** 1, 2005.
46. Kamakura, S., Oishi, K., Yoshimatsu, T., Nakafuku, M., Masuyama, N., and Gotoh, Y. Hes binding to STAT3 mediates crosstalk between Notch and JAK-STAT signalling. Nat Cell Biol **6,** 547, 2004.
47. De Strooper, B., and Annaert, W. Where Notch and Wnt signaling meet. The presenilin hub. J Cell Biol **152,** F17, 2001.
48. Imayoshi, I., Sakamoto, M., Yamaguchi, M., Mori, K., and Kageyama, R. Essential roles of Notch signaling in maintenance of neural stem cells in developing and adult brains. J Neurosci **30,** 3489, 2010.
49. Suzuki, I.K., Gacquer, D., Van Heurck, R., et al. Human-specific NOTCH2NL genes expand cortical neurogenesis through delta/notch regulation. Cell **173,** 1370.e16, 2018.
50. Fiddes, I.T., Lodewijk, G.A., Mooring, M., et al. Human-specific NOTCH2NL genes affect notch signaling and cortical neurogenesis. Cell **173,** 1356.e22, 2018.
51. Bejoy, J., Song, L., Wang, Z., Sang, Q.X., Zhou, Y., and Li, Y. Neuroprotective activities of heparin, heparinase III, and hyaluronic acid on the Aβ42-treated forebrain spheroids derived from human stem cells. ACS Biomater Sci Eng **4,** 2922, 2018.
52. Pasca, A.M., Sloan, S.A., Clarke, L.E., et al. Functional cortical neurons and astrocytes from human pluripotent stem cells in 3D culture. Nat Methods **12,** 671, 2015.
53. Dezonne, R.S., Sartore, R.C., Nascimento, J.M., et al. Derivation of functional human astrocytes from cerebral organoids. Sci Rep **7,** 45091, 2017.
54. Sloan, S.A., Darmanis, S., Huber, N., et al. Human astrocyte maturation captured in 3D cerebral cortical spheroids derived from pluripotent stem cells. Neuron **95,** 779.e6, 2017.
55. Gross, R.E., Mehler, M.F., Mabie, P.C., Zang, Z., Santschi, L., and Kessler, J.A. Bone morphogenetic proteins promote astroglial lineage commitment by mammalian subventricular zone progenitor cells. Neuron **17,** 595, 1996.
56. Xue, X., Sun, Y., Resto-Irizarry, A.M., et al. Mechanics-guided embryonic patterning of neuroectoderm tissue from human pluripotent stem cells. Nat Mater **17,** 633, 2018.
57. Marton, R.M., Miura, Y., Sloan, S.A., et al. Differentiation and maturation of oligodendrocytes in human three-dimensional neural cultures. Nat Neurosci **22,** 484, 2019.
58. Khakh, B.S., and Sofroniew, M.V. Diversity of astrocyte functions and phenotypes in neural circuits. Nat Neurosci **18,** 942, 2015.
59. Bradley, R.A., Shireman, J., McFalls, C., et al. Regionally specified human pluripotent stem cell-derived astrocytes exhibit different molecular signatures and functional properties. Development **146,** dev170910, 2019.
60. Li, X., Tao, Y., Bradley, R., et al. Fast generation of functional subtype astrocytes from human pluripotent stem cells. Stem Cell Rep **11,** 998, 2018.
61. Namihira, M., Kohyama, J., Semi, K., et al. Committed neuronal precursors confer astrocytic potential on residual neural precursor cells. Dev Cell **16,** 245, 2009.

Address correspondence to:
*Yan Li, PhD*
*Department of Chemical and Biomedical Engineering*
*FAMU-FSU College of Engineering*
*Florida State University*
*2525 Pottsdamer Street*
*Tallahassee, FL 32310*

*E-mail:* yli4@fsu.edu

*Received: August 1, 2019*
*Accepted: October 31, 2019*
*Online Publication Date: December 9, 2019*